Polar switching in the smectic-A_dP_A phase composed of asymmetric bent-core molecules

Lingfeng Guo,[1] Surajit Dhara,[2,*,†] B. K. Sadashiva,[3] S. Radhika,[3] R. Pratibha,[3] Yoshio Shimbo,[1] Fumito Araoka,[1] Ken Ishikawa,[1] and Hideo Takezoe[1,*,‡]

[1]*Department of Organic and Polymeric Materials, Tokyo Institute of Technology, O-okayama, Meguro-ku, Tokyo 152-8552, Japan*
[2]*School of Physics, University of Hyderabad, Hyderabad 500046, India*
[3]*Raman Research Institute, C. V. Raman Avenue, Bangalore 560080, India*

We have studied mesogenic properties in the smectic-A_dP_A phase of an asymmetric bent-core liquid crystal by means of polarizing optical microscopy, second-harmonic generation (SHG), electro-optical (EO), and dielectric measurements. In homeotropically aligned cells, EO switching is clearly observed from a schlieren texture with both four- and two-brush defects to a uniform bright domain under the application of very low in-plane electric field below 1 V/μm. The phase is SHG active under an electric field, i.e., SHG gradually increases without a threshold and saturates with the increasing field. In homogeneous cells, by applying triangular wave field at saturated voltage, the splitting of the polarization switching current peak is observed, indicating that the mesophase is antiferroelectric. The dielectric studies indicate a Debye-type relaxation of the transverse dipoles associated with the rotation of the molecules about their long axis. The dc bias-dependent dielectric relaxation time and the dielectric strength suggest that a field-induced antiferroelectric-ferroelectric phase transition occurs continuously beyond 1.2 V/μm and is reversible. The field-dependent texture observation is consistent with the dielectric measurements. Two possible models are proposed to interpret the continuous phase transition.

I. INTRODUCTION

Thermotropic liquid crystals composed of bent-shaped (banana-shaped) molecules exhibit a rich variety of phase structures and phase transitions [1,2]. Major attention has been paid to the polarity and chirality, i.e., polar layer structure due to the packing of bent-shape molecules and their switchability, and macroscopic chiral domains consisting of achiral molecules. In this paper, we focus on polar order and switching. As for phase structures, in addition to conventional banana phases such as B_1-B_8 [1], some smectic-A (Sm-A) family phases (orthogonal smectic phases) and biaxial nematic phase have been reported. Some of these phases show unique electro-optical (EO) and dielectric properties owing to the bent shape and their arrangement in the layer. Among them, the most extensively studied phase is the B_2 phase. In this phase, molecules are tilted from the smectic layer normal, so that two types of switching are possible, i.e., (1) conventional switching around cone preserving the layer chirality and (2) switching about molecular long axis [3,4]. The switching of type (2) is possible even in polar Sm-A (Sm-AP) phases, where layer polar order exists. We will focus on one of such phases in the present work.

Some bent-core molecules exhibit the conventional nonpolar uniaxial Sm-A phase. Another nonpolar but biaxial Sm-A_d phase, where molecules are interdigited in a smectic layer, has been reported [5–9]. Polar orthogonal phases, Sm-AP, were first reported by Eremin *et al.* [10]. They showed antiferroelectric switching, ascribed it to a bilayer antiferroelectric Sm-AP_A structure, where the free rotation about the longitudinal axis of molecules is hindered by the packing of bent-core molecules and neighboring layers have opposite bending (polarization) directions. Some other Sm-AP_A materials showing polar switching have also been reported [11–13]. Ferroelectric analog Sm-AP_F has also been reported [14]. Another interesting polar Sm-AP phase is the Sm-AP_R phase [15]. In this phase, dipoles form small polar domains, so that the phase is apparently uniaxial but exhibits polar switching. Considerable attention has been paid as a possible candidate for next-generation fast response display devices [16–18]. Here, we focus on the switchable Sm-A_dP_A phase which has an interdigited layer structure. The switching behavior in this phase has been reported earlier [7,11–13]. In the present study, we used a different compound, which shows the Sm-A_dP_A phase, and found electric-field-induced thresholdless antiferroelectric-ferroelectric transition. Similar continuous transition has ever been observed in tilted smectic phases previously [19,20], but not in the nontilted phase. Further, in this phase chiral domains were also observed in an orthogonal system composed of achiral molecules. A variety of experimental results and possible switching models is described.

II. EXPERIMENTAL

The sample used in this study was an asymmetric bent-core molecule with a longitudinal strong dipole (C≡N) and a flexible alkyl chain at one end, as shown in Fig. 1(a). The details of the synthetic scheme and chemical properties will be reported elsewhere. This compound shows the following phase sequence: crystal (Cr)-134.8 °C-Sm-A_dP_A-149.0 °C-Sm-A_d-150.2 °C-Isotropic (Iso) on heating and Iso-149.5 °C-Sm-A_d-148.3 °C-Sm-A_dP_A-112.6 °C-Cr on

*Corresponding author.
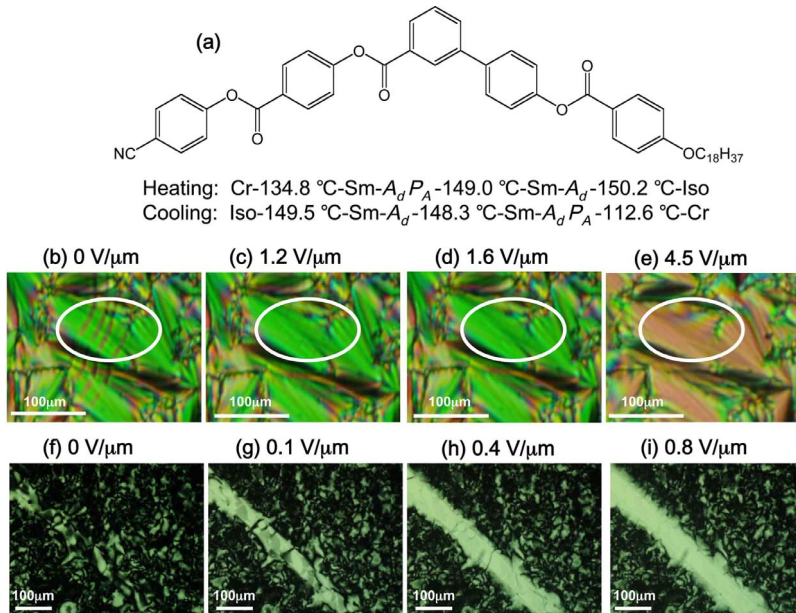†sdsp@uohyd.ernet.in
‡takezoe.h.aa@m.titech.ac.jp

Heating: Cr-134.8 °C-Sm-A_dP_A-149.0 °C-Sm-A_d-150.2 °C-Iso
Cooling: Iso-149.5 °C-Sm-A_d-148.3 °C-Sm-A_dP_A-112.6 °C-Cr

FIG. 1. (Color online) (a) Chemical structure and phase sequence of the compound used in the experiment. (b)–(e) Planar texture of a 12.8-μm-thick cell at 145 °C under various vertical dc fields. (f)–(i) Homeotropic texture of a 5.6-μm-thick cell at 138 °C under various in-plane dc fields.

cooling. For preparing planar cells, glass plates coated with indium tin oxide were spin coated with polyimide (JSR, AL-1254) and cured at 180 °C for 1 h. The plates were rubbed antiparallel to obtain homogeneous alignment of the director. In homeotropic cells, polyimide (Nissan Chemical, SE-1211) was used as an alignment layer. A uv curable adhesive mixed with spacer was used to make cells of typical thickness. The sample was filled in empty cells in the isotropic phase by capillary action and cooled slowly.

Texture observations were made by using a polarizing optical microscope (Nikon, Optiphot-pol) equipped with a hot stage and temperature controller (Mettler Toledo FP 82). A function generator connected with a high voltage amplifier was used to study the electro-optical switching behavior. The polarization reversal current was measured across a 1 MΩ resistor using a standard triangular wave technique. The second-harmonic generation (SHG) measurements were also conducted using a planar cell. The light intensity of the fundamental light, Nd:YAG laser (1064 nm, 8 ns duration, and 10 Hz repetition), was reduced down to 6 mJ/mm^2 and was incident into the sample at 45° incidence. The SHG signal was detected in the transmission direction by a photomultiplier tube (Hamamatsu, R955) after blocking the fundamental light by IR cut and interference filters. The signal was accumulated for 30 s with a boxcar integrator (Stanford Research Systems, SR-250). A frequency response analyzer (Solartron 1255B) with a dielectric interface (Solartron 1296) was used to measure the dielectric properties in a homogeneously aligned cell. The measuring field was 0.3 V$_{pp}$ and a dc biased field up to 40 V was applied. The real and imaginary parts of the dielectric permittivity from 1 Hz to 1 MHz were measured under different bias fields.

III. RESULTS

Let us show texture changes upon electric field application in the Sm-A_dP_A phase under crossed polarizers. Figures 1(b)–1(i) show the results for homogeneous (at 145 °C) and homeotropic (at 138 °C) cells, respectively. Homogeneously aligned samples show a fan-shaped texture. A few stripes existed in the absence of a field [Fig. 1(b)], disappeared by applying a small field [Figs. 1(c) and 1(d)], and obvious birefringence change was followed under a higher field like 4.5 V/μm [Fig. 1(e)]. We found that birefringence color change was continuous, and the textural change was reversible. We also conducted x-ray diffraction experiments under an applied field and no noticeable change in the layer spacing was observed, indicating that the antiferroelectric to ferroelectric transition occurs keeping the layer spacing unchanged. In homeotropically aligned cells, a schlieren texture with both four- and two-brush defects were observed [Fig. 1(f)]. An in-plane electric field was applied across a gap of 50 μm, where the electric field was 45° to crossed polarizers, and the temperature was fixed at 138 °C. By applying a field, the texture changed continuously [Figs. 1(g) and 1(h)] and became uniformly bright [Fig. 1(i)] even under very low voltage (below 1 V/μm). During the whole process, no threshold could be observed.

We now show SHG results as a function of temperature and electric field. In the absence of an electric field, no SHG signal was observed in the whole temperature range, implying that this phase has no macroscopic polar domains. On the other hand, by applying a rectangular wave field to planar cells, comparatively strong SH signal was detected in the Sm-A_dP_A phase both in heating and cooling runs. The electric-field-dependent SHG signal is shown in Fig. 2(a). The measurement was carried out at 140 °C in a cooling process in an 8.9 μm cell. The SH signal gradually increased with increasing field and saturated above 120 V$_{pp}$. Note that no distinct threshold voltage could be observed in the SHG intensity change. Figure 2(b) shows the temperature dependence of the SH signal under a rectangular wave voltage of 80 V$_{pp}$. In the cooling process, the SH signal emerged quickly from zero and showed a maximum value when the transition to the Sm-A_dP_A occurred. Then the signal gradu-
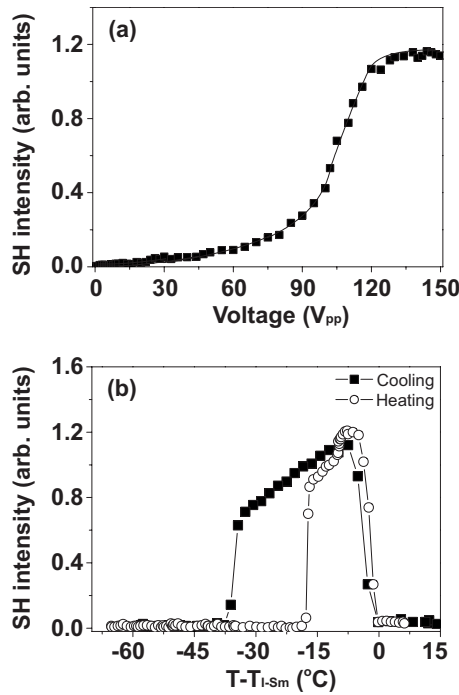
FIG. 2. (a) SHG intensity as a function of applied voltage at 140 °C. (b) SHG intensity as a function of temperature in both cooling (squares) and heating (open circles) runs in a homogeneous sample at an applied rectangular voltage of 80 V_{pp} and at a frequency of 10 Hz. Cell thickness is 8.9 μm.

FIG. 3. (a) Switching current in the Sm-A_dP_A phase by applying a triangular wave voltage of 120 V_{pp} and with the frequency of 9 Hz at 138 °C. (b) Spontaneous polarization (P_s) as a function of temperature. Cell thickness is 4.8 μm.

ally decreased with reducing temperature. The gradual decrease could be explained by the increase in scattering caused by rigid boundaries of local domains on cooling. The SHG intensity drops to zero upon crystallization. Similar tendency was also observed in the heating procedure. We note, however, that the temperature-dependent behavior changes with an applied field since the saturation field depends on temperature. Figure 2(b) is one of the typical examples.

We measured the polarization reversal current in a 4.8-μm-thick planar cell at various temperatures to identify the switching behavior. The applied field was a triangular wave voltage of 120 V_{pp} and frequency of 9 Hz. At 138 °C, double switching current peaks were detected, as shown in Fig. 3(a), indicating that the ground-state structure of the mesophase is antiferroelectric. Two current peaks are closely located at about 0 V. This behavior is consistent to the quasicontinuous ferroelectric transition shown by the SHG measurement [Fig. 2(a)]. Similar continuous field-induced antiferroelectric-ferroelectric transitions were detected in tilted smectic phases by applying simple and modified triangular wave fields [19,20]. However, such a continuous antiferroelectric-ferroelectric transition has never been observed in the orthogonal smectic phase such as the Sm-A_dP_A phase. The variation of spontaneous polarization (P_s) as a function of temperature is shown in Fig. 3(b). The P_s value increases rapidly from ~60 nC/cm^2 to around 260 nC/cm^2 after the transition to the polar phase and drops sharply to zero at crystallization.

The dielectric properties were measured as a function of frequency from 1 Hz to 1 MHz at various temperatures. The
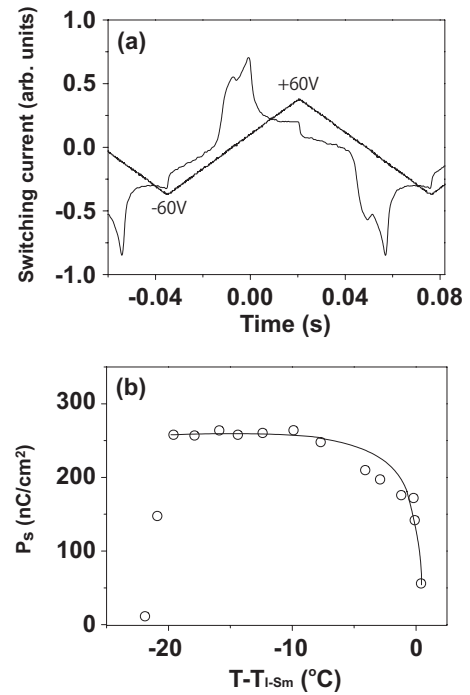
real part (ε') and imaginary part (ε'') are given in Figs. 4(a) and 4(b), respectively. It is noticed that in the isotropic phase ($T-T_{I-Sm}=+1$) only one low-frequency ionic relaxation is observed near 20 Hz. In the Sm-A_dP_A phase there is another relaxation near 100 kHz and it is temperature dependent. In order to confirm that the low-frequency relaxation is due to the ionic relaxation, we increased the dc bias voltage up to
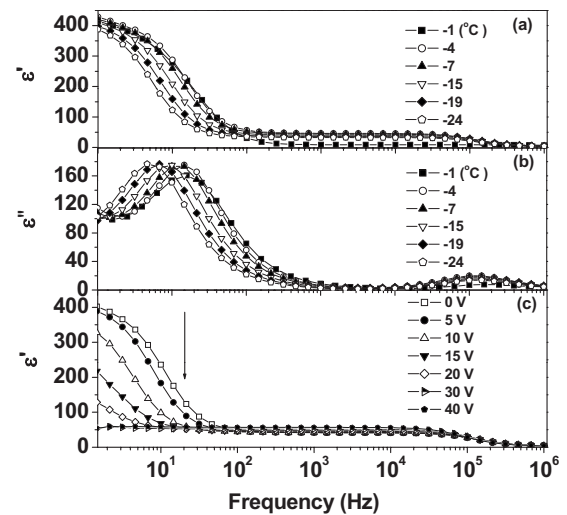

FIG. 4. Dielectric permittivity in the Sm-A_dP_A phase. (a) Real part (ε') and (b) imaginary part (ε'') as functions of frequency at various relative temperatures ($T-T_{I-Sm}$). (c) The effect of dc bias field on the dielectric constant (ε') at $T-T_{I-Sm}=-10$ °C. Cell thickness is 12.8 μm.
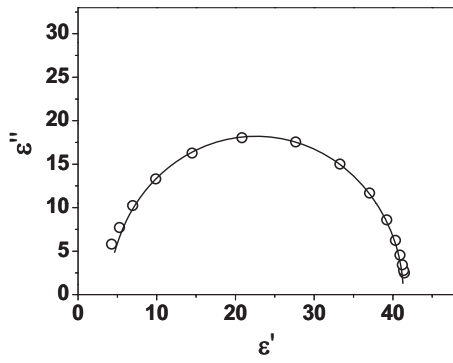
FIG. 5. Cole-Cole plot of the dielectric permittivity at 138 °C.

FIG. 7. Variation of relaxation time τ (squares) and the dielectric strength $\Delta\varepsilon$ (open circles) as a function of dc bias field.

40 V and found that the low-frequency dielectric constant reduced and the ionic relaxation could be suppressed almost completely as the ions were swept away from the bulk under dc bias fields as seen in Fig. 4(c). On the contrary, another relaxation at about 100 kHz was enhanced by increasing the bias voltage (see Fig. 7 later). The Cole-Cole plot of real (ε') and imaginary (ε'') parts of the dielectric constants at the temperature of 138 °C is shown in Fig. 5. As we mentioned that the low-frequency dielectric relaxation is due to the ion, we used data from 100 Hz to 1 MHz to describe the dielectric relaxation. Single semicircular arc clearly suggests that there is only one relaxation and further it is Debye type as the data are well fitted with the Debye equation. Thus, we use the Debye equation to analyze the frequency-dependent
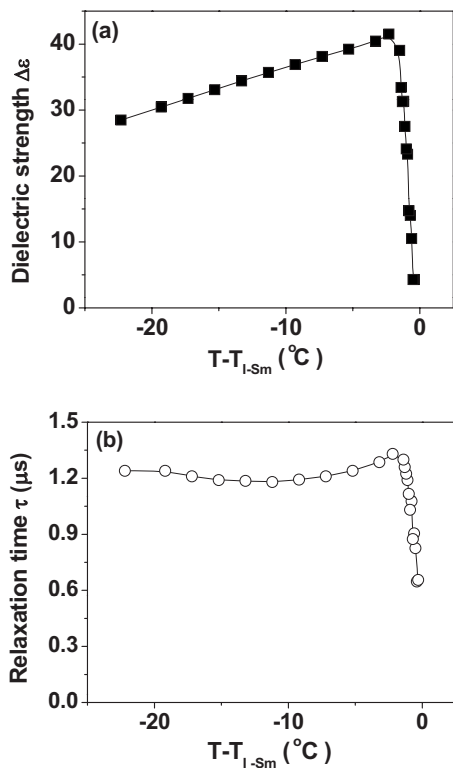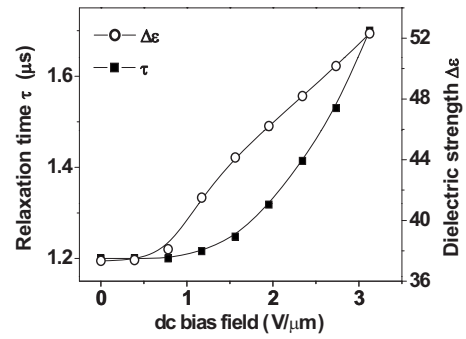
dielectric data at various temperatures and dc bias fields. The dielectric strength ($\Delta\varepsilon$) and the dielectric relaxation time (τ) were obtained as fitting parameters.

The variation of the dielectric strength as a function of temperature is shown in Fig. 6(a). It is seen that the dielectric strength increases rapidly from 4 in the isotropic phase and attain a maximum at the Sm-A_d to Sm-A_dP_A transition. The value of $\Delta\varepsilon$ decreases slightly as the temperature is lowered due to the gradual increase in viscosity in the cooling process. From Fig. 6(b) it is noticed that the relaxation time (τ) also rapidly increases from 0.6 μs to about 1.3 μs in the vicinity of Sm-A_d–Sm-A_dP_A phase transition and in the Sm-A_dP_A phase it is almost independent of temperature. Such a rapid increase of τ in Sm-A_dP_A phase is due to the rapid growth of the polar order. The average polarization direction is along the bending direction and is parallel to the layer. The relaxation at about 100 kHz is attributed to that of the molecular motion associated with this polarization response. Figure 7 shows the effect of dc bias field on this relaxation mode. It is discerned that relaxation strength and relaxation time are almost constant up to 1.2 V/μm. When the voltage continues to rise, both of them progressively increase with the electric field. It can be explained as follows: by applying a dc field, macroscopic polarization emerges by distorting the antiferroelectric structure to the ferroelectric one, so that the dielectric strength increases.

FIG. 6. Variation of (a) dielectric strength ($\Delta\varepsilon$) and (b) relaxation time (τ) as a function of relative temperatures.
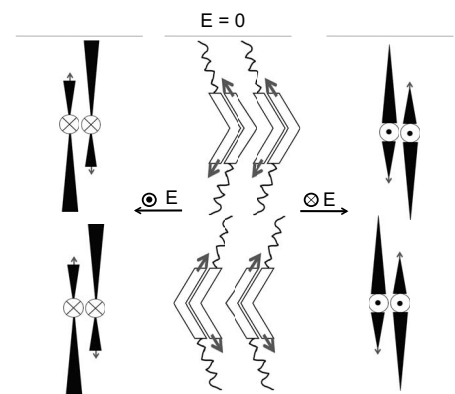

FIG. 8. Simple model of the field-induced antiferroelectric-ferroelectric transition. Black arrows connected to the arms of bent cores stand for the stronger dipole of C≡N.
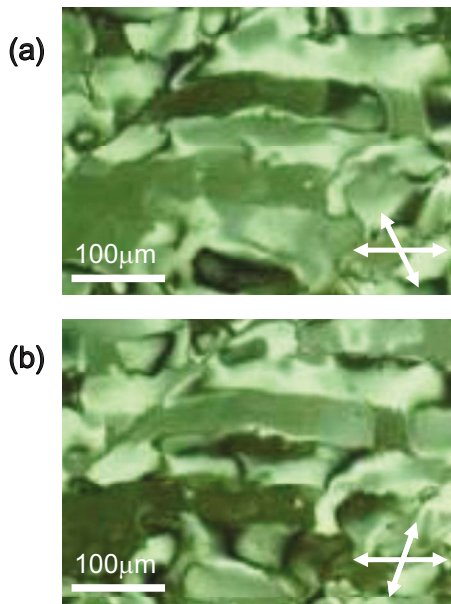
FIG. 9. (Color online) (a) and (b) Homeotropic textures under polarizers decrossed in the opposite direction. White arrows represent polarizer and analyzer. The dark regions with their brightness interchanged by rotating the analyzer clockwise or counterclockwise are chiral domains.

Similar phenomenon has been observed in the antiferroelectric smectic-C^* (Sm-CA^*) [21].

IV. DISCUSSION

Now we consider a possible model of EO switching based on x-ray, EO, and SHG studies. We believe the previous model of molecular packing proposed by Sadashiva *et al.* [6], as shown in Fig. 8 (middle). In the absence of a field, the bent cores of molecules are parallel to substrate surfaces because of an electrostatic interaction between molecules and surfaces as well as packing entropy effect. This model is reasonable from x-ray analysis data, i.e., the calculated individual molecular length L is 46.4 Å, while the layer thickness experimentally obtained is 54.5 Å, suggesting an interdigited structure. Moreover, this arrangement satisfies compact packing of bent cores. In this arrangement, the polarization component along the layer normal is totally cancelled, whereas macroscopic layer polarization emerges parallel to the layer. Because of the antiferroelectric orientation, this layer polarization is also cancelled between adjacent layers, so that no macroscopic polarization can be detected without applying an electric field, being consistent to non-SHG activity. However, when an external field is applied on the sample, the layer polarization reorients toward the field direction, as shown in Fig. 8, i.e., the paired molecules rotate about their molecular long axis or the layer normal. It is clear that the birefringence increases by applying an electric field, being consistent to the texture change shown in Figs. 1(b)–1(e).

Usually field-induced antiferroelectric-ferroelectric transition is associated with the threshold behavior both in classical Sm-CA^* [22] and bent-core B_2 [23] phases. In the present case, however, all the measurements indicate the thresholdless behavior. We can suggest two ideas to explain this behavior. (1) The potential barrier between the antiferroelectric and ferroelectric states is so low that electric-field-induced transition occurs quasicontinuously. This idea is supported by closely located double switching current peaks as shown in Fig. 3(a). (2) The existence of helical structure. Actually we observed spontaneous formation of chiral domains, as shown in Fig. 9. In these textures of homeotropically aligned cells under decrossed polarizers, the brightness of some areas interchanged by slightly rotating an analyzer clockwise or counterclockwise, indicating the existence of chiral domains.

The phenomenon is similar to the spontaneous chiral domain formation observed in the B_4 [24] and dark conglomerate [25] phases. However, the phase shown by the present sample is a fluid phase, being quite different from B_4 and dark conglomerate phases. So far, the spontaneous chiral domain formation has also been reported in nonchiral fluid nematic phase [26–29]. However, these chiral domain formations were recently ascribed to surface effect [30]. In the present case, however, the situation is very different because of the following reasons: (1) we used homeotropic cells, so that the surface anchoring must be very weak, and (2) the chiral domains are very unstable. The shape of domains is easily changed by slightly changing temperature and lightly touching even the oven, where our sample is located. Hence, we can conclude that the chiral domain formation in our sample is not caused by surfaces.

Moreover, the observed phenomenon is slightly different: besides the chiral domains, which show brightness change in oppositely decrossed polarizers, there exist bright areas, which show no significant change under uncrossed polarizers. In this nontilted (orthogonal) Sm-A_dP_A phase, the longitudinal axis is parallel to the layer normal and the polar direction lies in the layer planes. Therefore, there are two twofold rotation axes along the polar (bending) direction and perpendicular to it at the layer boundaries. In addition bending plane is a mirror plane, so that the local structure of the Sm-A_dP_A phase has D_{2h} symmetry. For the Sm-A_dP_A phase to be chiral, a helical structure must be formed. Therefore, three domains, two chiral and one nonchiral, are attributed to right- and left-handed helix and nonhelical domains, respectively. By applying an electric field, helix unwinding and antiferroelectric to ferroelectric deformation take place at the same time. This may be the reason why the threshold of the field-induced antiferroelectric-ferroelectric is not so distinct. Further studies are necessary to clarify the helical structure.

V. CONCLUSIONS

We characterized the Sm-A_dP_A phase of an asymmetric bent-core liquid crystal by means of polarizing optical microscopy, SHG, EO, x-ray, and dielectric measurements. The compound is SHG active under electric field and a characteristic dielectric relaxation appears at about 100 kHz attributed to the rotation of the molecules about the long axis. The dc field enhances this dielectric relaxation, suggesting the polar order nucleated by the dc bias effect. The field-induced antiferroelectric-ferroelectric (Sm-A_dP_A–Sm-A_dP_F) transi-

tion occurs continuously without a distinct threshold. We suggested two possible models to interpret this continuous transition, i.e., very low barrier between the two phases and the existence of helical structure. Both ideas are supported by the present experiments.

[1] H. Takezoe and Y. Takanishi, Jpn. J. Appl. Phys., Part 1 **45**, 597 (2006).

[2] R. Amaranatha Reddy and C. Tschierske, J. Mater. Chem. **16**, 907 (2006).

[3] R. Amaranatha Reddy, M. W. Schröder, M. Bodyagin, H. Kresse, S. Diele, G. Pelzl, and W. Weissflog, Angew. Chem., Int. Ed. **44**, 774 (2005).

[4] M. Nakata, R.-F. Shao, J. E. Maclennan, W. Weissflog, and N. A. Clark, Phys. Rev. Lett. **96**, 067802 (2006).

[5] B. K. Sadashiva, R. Amaranatha Reddy, R. Pratibha, and N. V. Madhusudana, Chem. Commun. (Cambridge) 2140 (2001).

[6] B. K. Sadashiva, R. Amaranatha Reddy, R. Pratibha, and N. V. Madhusudana, J. Mater. Chem. **12**, 943 (2002).

[7] R. Amaranatha Reddy and B. K. Sadashiva, J. Mater. Chem. **14**, 310 (2004).

[8] C. V. Yelamaggad, I. S. Shashikala, D. S. S. Rao, G. G. Nair, and S. K. Prasad, J. Mater. Chem. **16**, 4099 (2006).

[9] C. V. Yelamaggad, I. S. Shashikala, V. P. Tamilenthi, D. S. S. Rao, G. G. Nair, and S. K. Prasad, J. Mater. Chem. **18**, 2096 (2008).

[10] A. Eremin, S. Diele, G. Pelzl, H. Nadasi, W. Weissflog, J. Salfetnikova, and H. Kresse, Phys. Rev. E **64**, 051707 (2001).

[11] U. Dunemann, M. W. Schroder, R. Amaranatha Reddy, G. Pelzl, S. Diele, and W. Weissflog, J. Mater. Chem. **15**, 4051 (2005).

[12] D. Pociecha, E. Gorecka, M. Cepic, N. Vaupotic, and W. Weissflog, Phys. Rev. E **74**, 021702 (2006).

[13] H. N. Shreeninvasa Murthy and B. K. Sadashiva, Liq. Cryst. **31**, 567 (2004).

[14] R. Shao *et al.*, 22nd International Liquid Crystal Conference, Jeju, Korea, 2008 (unpublished).

[15] D. Pociecha, M. Cepic, E. Gorecka, and J. Mieczkowski, Phys. Rev. Lett. **91**, 185501 (2003).

[16] Y. Shimbo, Y. Takanishi, K. Ishikawa, E. Gorecka, D. Pochiecha, J. Mieczkowski, K. Gomola, and H. Takezoe, Jpn. J. Appl. Phys., Part 2 **45**, L282 (2006).

[17] Y. Shimbo, E. Gorecka, D. Pociecha, F. Araoka, M. Goto, Y. Takanishi, K. Ishikawa, J. Mieczkowski, K. Gomola, and H. Takezoe, Phys. Rev. Lett. **97**, 113901 (2006).

[18] K. Gomola, L. Guo, S. Dhara, Y. Shimbo, E. Gorecka, D. Pociecha, J. Mieczkowski, and H. Takezoe, J. Mater. Chem. **19**, 4240 (2009).

[19] C. Keith, R. Amaranatha Reddy, U. Baumeister, H. Hahn, H. Lang, and C. Tschierske, J. Mater. Chem. **16**, 3444 (2006).

[20] M. F. Achard, J. Ph. Bedel, J. P. Marcerou, H. T. Nguyen, and J. C. Rouillon, Eur. Phys. J. E **10**, 129 (2003).

[21] K. Hiraoka, H. Takezoe, and A. Fukuda, Ferroelectrics **147**, 13 (1993).

[22] A. D. L. Chandani, T. Hagiwara, Y. Suzuki, Y. Ouchi, H. Takezoe, and A. Fukuda, Jpn. J. Appl. Phys., Part 2 **27**, L729 (1988).

[23] K. Kumazawa, M. Nakata, F. Araoka, Y. Takanishi, K. Ishikawa, J. Watanabe, and H. Takezoe, J. Mater. Chem. **14**, 157 (2004).

[24] J. Thisayukta, H. Takezoe, and J. Watanabe, Jpn. J. Appl. Phys., Part 1 **40**, 3277 (2001).

[25] S. Kang, Y. Saito, N. Watanabe, M. Tokita, Y. Takanishi, H. Takezoe, and J. Watanabe, J. Phys. Chem. B **110**, 5205 (2006).

[26] G. Pelzl, A. Eremin, S. Diele, H. Kresse, and W. Weissflog, J. Mater. Chem. **12**, 2591 (2002).

[27] T. Niori, J. Yamamoto, and H. Yokoyama, Mol. Cryst. Liq. Cryst. **409**, 475 (2004).

[28] V. Görtz and J. W. Goodby, Chem. Commun. (Cambridge) 3262 (2005).

[29] C. Präsang, A. C. Whitwood, and D. W. Bruce, Chem. Commun. (Cambridge) 2137 (2008).

[30] P. S. Salter, P. W. Benzie, R. A. Reddy, C. Tschierske, S. J. Elston, and E. P. Raynes, Phys. Rev. E **80**, 031701 (2009).